The EMBO Journal (2008) 27, 2471–2483 | © 2008 European Molecular Biology Organization | All Rights Reserved 0261-4189/08
www.embojournal.org

THE EMBO JOURNAL

LIS1 and NDEL1 coordinate the plus-end-directed transport of cytoplasmic dynein

Masami Yamada[1,9], Shiori Toba[2,8,9], Yuko Yoshida[1], Koji Haratani[1], Daisuke Mori[1], Yoshihisa Yano[1], Yuko Mimori-Kiyosue[3], Takeshi Nakamura[4], Kyoko Itoh[5], Shinji Fushiki[5], Mitsutoshi Setou[6], Anthony Wynshaw-Boris[7], Takayuki Torisawa[2], Yoko Y Toyoshima[2] and Shinji Hirotsune[1,*]

[1]Department of Genetic Disease Research, Osaka City University Graduate School of Medicine, Osaka, Japan, [2]Department of Life Sciences, Graduate School of Arts and Sciences, The University of Tokyo, Tokyo, Japan, [3]Research Group for Cytoskeleton & Cell Motility, KAN Research Institute Inc., Kobe, Japan, [4]Laboratory of Bioimaging and Cell Signaling, Graduate School of Biostudies, Kyoto University, Kyoto, Japan, [5]Department of Pathology and Applied Neurobiology, Kyoto Prefectural University of Medicine Graduate School of Medical Sciences, Kyoto, Japan, [6]Department of Molecular Anatomy, Hamamatsu University School of Medicine, Shizuoka, Japan and [7]Department of Pediatrics and Institute for Human Genetics, UCSF School of Medicine, San Francisco, CA, USA

LIS1 was first identified as a gene mutated in human classical lissencephaly sequence. LIS1 is required for dynein activity, but the underlying mechanism is poorly understood. Here, we demonstrate that LIS1 suppresses the motility of cytoplasmic dynein on microtubules (MTs), whereas NDEL1 releases the blocking effect of LIS1 on cytoplasmic dynein. We demonstrate that LIS1, cytoplasmic dynein and MT fragments co-migrate anterogradely. When LIS1 function was suppressed by a blocking antibody, anterograde movement of cytoplasmic dynein was severely impaired. Immunoprecipitation assay indicated that cytoplasmic dynein forms a complex with LIS1, tubulins and kinesin-1. In contrast, immunoabsorption of LIS1 resulted in disappearance of co-precipitated tubulins and kinesin. Thus, we propose a novel model of the regulation of cytoplasmic dynein by LIS1, in which LIS1 mediates anterograde transport of cytoplasmic dynein to the plus end of cytoskeletal MTs as a dynein–LIS1 complex on transportable MTs, which is a possibility supported by our data.

The EMBO Journal (2008) **27,** 2471–2483. doi:10.1038/emboj.2008.182; Published online 11 September 2008
Subject Categories: membranes & transport; cell & tissue architecture
Keywords: dynein; LIS1; lissencephaly

*Corresponding author. Department of Genetic Disease Research, Osaka City University Graduate School of Medicine, Asahi-machi 1-4-3 Abeno, Osaka 545-8585, Japan. Tel.: +81 6 6645 3725; Fax: +81 6 6645 3727; E-mail: shinjih@med.osaka-cu.ac.jp
[8]Present address: Kobe Advanced ICT Research Center, National Institute of Information and Communications Technology, Kobe, Japan
[9]These authors contributed equally to this work

Received: 16 January 2008; accepted: 14 August 2008; published online: 11 September 2008

Introduction

The formation of the complex architecture of the mammalian cerebral cortex requires the orchestrated movement of neuronal cells arising from different regions within the brain, and born at different times, to achieve specific laminar positions, orientation and connections with other cells (Gupta *et al*, 2002). Mutations of genes involved in cell movements result in various defects of corticogenesis. Classical lissencephaly represents one of the most severe disorders of neocortical neuronal migration. It is characterized by a paucity of cortical gyration accompanied by thickening of the cortex (Dobyns *et al*, 1991, 1993). Heterozygous mutation in *platelet-activating factor acetylhydrolase 1B α subunit* (PAFAH1B1, encoding sthe LIS1 protein) is one of the major causes of classical lissencephaly (Dobyns *et al*, 1991, 1993). LIS1 is a highly evolutionarily conserved protein that also includes NudF in *Aspergillus nidulans*, Pac1 in *Saccharomyces cerevisiae* and Dlis1 in *Drosophila melanogaster* (Morris *et al*, 1998; Efimov and Morris, 2000; Faulkner *et al*, 2000; Lei and Warrior, 2000; Lee *et al*, 2003). In all of the organisms where they have been examined, LIS1 orthologues are complexed with cytoplasmic dynein, the main cytoplasmic microtubule (MT) 'minus'-end-directed motor.

LIS1-binding proteins, NDEL1 and NDE1 are also complexed with cytoplasmic dynein (Feng *et al*, 2000; Niethammer *et al*, 2000; Sasaki *et al*, 2000). NDEL1 and NDE1 are mammalian NudE homologues, which was identified as multicopy suppressors of a mutation in the nudF gene (Efimov and Morris, 2000). *Lis1* or *Ndel1* disrupted mice displayed neuronal migration defects, and in addition, double mutants exhibited more severe neuronal migration defects than each mutant, suggesting that *Lis1* and *Ndel1* genetically interact and are present in a common pathway as a regulator of cytoplasmic dynein (Hirotsune *et al*, 1998; Sasaki *et al*, 2005).

In migrating neurons, the centrosome is positioned ahead of the nucleus, with MTs forming a perinuclear cage-like structure converging into the centrosome and projecting into the leading process from the centrosome (Rivas and Hatten, 1995). MT structures couple the leading process to the centrosome and the centrosome to the nucleus to translocate the nucleus (nucleus–centrosome (N–C) coupling). *Lis1*+/− neurons displayed increased and more variable separation between the nucleus and the preceding centrosome during migration, whereas cytoplasmic dynein inhibition resulted in similar defects in both N–C coupling and neuronal migration (Tanaka *et al*, 2004). Loss of function of LIS1, NDEL1 or cytoplasmic dynein in developing neocortex by siRNA also impairs neuronal positioning and causes the uncoupling of N–C coupling (Shu *et al*, 2004). These and other observations support the notion that LIS1 and NDEL1 are essential for the proper function of cytoplasmic dynein. A vital role of LIS1 and NDEL1 for the regulation of cytoplasmic dynein is adapted in non-neuronal cells. For example,

overexpression of LIS1 in cultured mammalian cells interferes with mitotic progression and leads to spindle misorientation. Injection of anti-LIS1 antibody interferes with attachment of chromosomes to the metaphase plate, and leads to chromosome loss (Faulkner *et al*, 2000). Cytoplasmic dynein and LIS1 localize to the leading cell cortex during healing of wounded cells. Inhibition of dynein and LIS1 interferes not only with reorientation of the MT network but also with persistent directed cell migration as well (Dujardin *et al*, 2003).

Although these and other reports clearly indicate that LIS1 and NDEL1 are regulating cytoplasmic dynein, the molecular mechanism by which LIS1 and NDEL1 control cytoplasmic dynein function remains unknown. Here, we report that LIS1 suppresses the motility of cytoplasmic dynein, and holds cytoplasmic dynein on MTs, whereas NDEL1 releases the blocking effect of LIS1 on cytoplasmic dynein, allowing cytoplasmic dynein to be active in the presence of LIS1. When LIS1 was blocked by an anti-LIS1 antibody, anterograde movement of cytoplasmic dynein was severely impaired. Immunoprecipitation/immunoabsorption assays revealed that LIS1 is required for assembling cytoplasmic dynein with tubulins. We further demonstrated that LIS1, cytoplasmic dynein and tubulins co-migrate anterogradely in the cell. We present a novel model of the regulation of cytoplasmic dynein by LIS1 within the cell, in which LIS1 mediates plus-end-directed transport of cytoplasmic dynein as a complex consisting of cytoplasmic dynein, LIS1 and tubulins.

Results

LIS1 holds cytoplasmic dynein on the MTs, whereas NDEL1 releases cytoplasmic dynein

To elucidate the molecular mechanism of dynein regulation by LIS1 and NDEL1, we performed *in vitro* studies using purified native dynein and recombinant LIS1 and NDEL1 expressed in insect cells (Toyo-Oka *et al*, 2005). Native dynein, purified from porcine brain by the temperature-dependent assembly and disassembly cycles and anion exchange chromatography (Bingham *et al*, 1998; Toba and Toyoshima, 2004), is composed of heavy, intermediate, light intermediate and light chains, but free from LIS1 and NDEL1 (Supplementary Figure 1A and B). Sedimentation experiments indicated that LIS1 and NDEL1 each directly bind to dynein, and that both proteins together bind to dynein in nearly equal molar ratios (Supplementary Figure 1C).

Purified dynein translocated MTs in an *in vitro* motility assay where MTs glide on a dynein-coated surface as reported earlier (Paschal *et al*, 1987; Vale and Toyoshima, 1988; Vallee *et al*, 1988; Toba and Toyoshima, 2004), demonstrating that LIS1 and NDEL1 are not essential components for the motility of dynein (Figure 1A). We then examined the effects of LIS1 and NDEL1 on dynein motor activity. When dynein was mixed with different amounts of LIS1 and then introduced into the observation chamber, increasing amounts of LIS1 gradually decreased the MT gliding speed (Figure 1A) and eventually stopped MT gliding altogether, indicating that LIS1 negatively regulates the motility of dynein in a dose-dependent manner. When LIS1 alone was applied to the observation chamber without dynein, MTs were not associated with the glass surface (data not shown), suggesting that the impairment of MT gliding by LIS1 was attributed to the direct blocking of dynein motility by LIS1 rather than tethering of MTs to the glass surface by LIS1. Next, we examined the effects of NDEL1, and found that at lower concentrations, the MT gliding speed did not change appreciably, but the number of MTs associated with the surface decreased (Figure 1A). At a high concentration of NDEL1 (30-fold stoichiometric amount to dynein in the mixture), no MTs were bound to dynein on the glass surface, indicating that NDEL1 facilitates the dissociation of dynein from MTs. Thus, both LIS1 and NDEL1 impaired dynein-mediated gliding of MTs but by different mechanisms. These results are unexpected from previous reports demonstrating the roles of LIS1 and NDEL1 as an activator and a regulator of dynein function (Shu *et al*, 2004; Mesngon *et al*, 2006). We next examined the effect of the presence of both LIS1 and NDEL1 on dynein motility. Remarkably, these two proteins together restored dynein motility to the control level, although each protein individually impaired dynein motility (Figure 1A). This effect was not caused by the dissociation of both the proteins from dynein, because sedimentation analysis revealed that both LIS1 and NDEL1 were associated together with dynein (Supplementary Figure 1C). To exclude the possibility of an artificial effect from the GST tag, assays were performed with GST-truncated proteins with the same results (Supplementary Figure 1D and E). We further performed motility assays with either a blocking antibody against LIS1 or a blocking antibody against NDEL1 (see below). The presence of blocking antibody clearly abolished the effect of LIS1 or NDEL1 on the motility of cytoplasmic dynein, supporting the interpretation that the LIS1 or NDEL1 effect on cytoplasmic dynein is attributed to the specific effect of LIS1 or NDEL1 protein. Thus, we concluded that LIS1 suppresses the motility of dynein, whereas NDEL1 releases the suppression of dynein motility by LIS1.

We next examined whether LIS1 and NDEL1 affected the ATPase activity of dynein. The ATPase activity of dynein was increased approximately five-fold in the presence of MTs. LIS1 slightly enhanced ATPase activity at concentrations that inhibit dynein motility (Figure 1B), suggesting that LIS1 breaks the mechano-chemical coupling of dynein. In contrast, NDEL1 reduced the MT-stimulated ATPase activity of dynein to about 60% of control levels, a result consistent with the observation that NDEL1 facilitates the dissociation of dynein from MTs. Intriguingly, the MT-activated ATPase activity in the presence of both LIS1 and NDEL1 was restored to the same level as control dynein, suggesting that NDEL1 reversed the LIS1 blocking of the mechano-chemical coupling of dynein.

We also performed MT-binding assays to address the function of LIS1 and NDEL1 on the binding of cytoplasmic dynein with MTs. The results from MT binding of dynein and LIS1/NDEL1 (Figure 1C) further supported the data from the motility and ATPase assays. More dynein precipitated in the presence of LIS1. In contrast, more dynein appeared in the supernatant in the presence of NDEL1, indicating that NDEL1 binding weakens the affinity of dynein for MTs.

LIS1 is essential for plus-end-directed transport of dynein

Cytoplasmic dynein is the minus-end-directed motor protein responsible for transport of various cell components from the

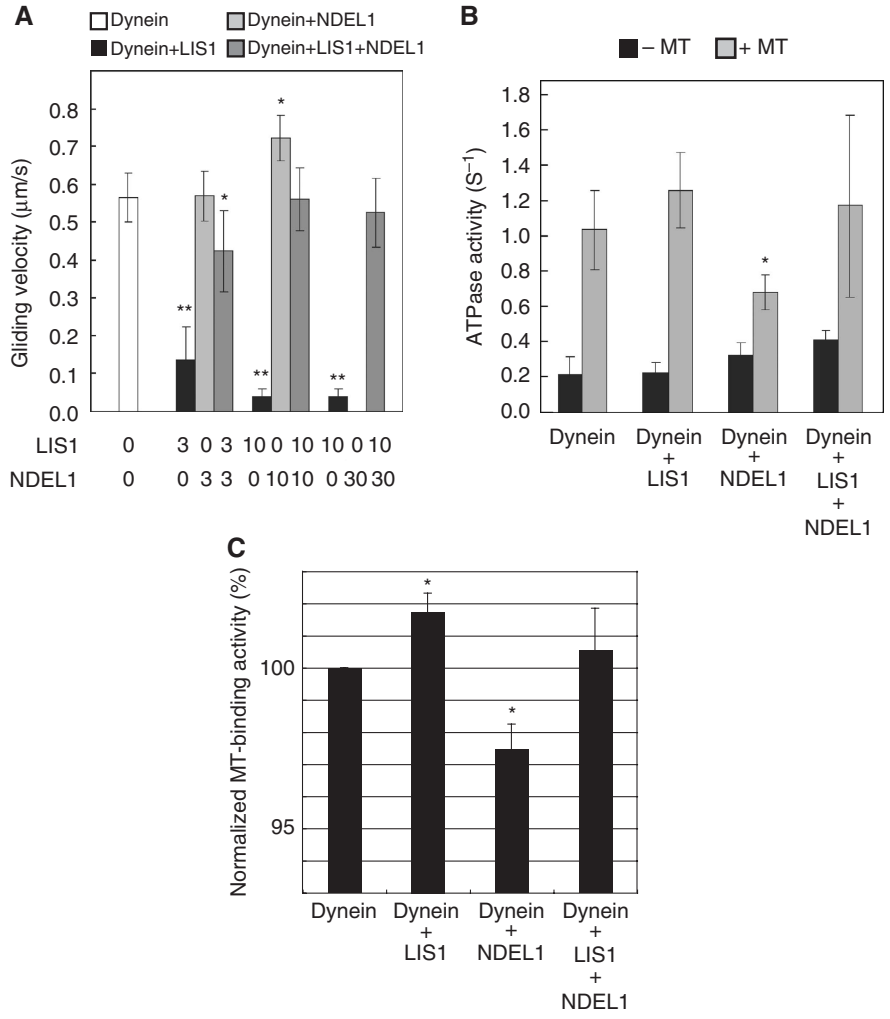

	Experiment 1	Experiment 2	Experiment 3	Average±s.d.
Dynein	100	100	100	100
Dynein+LIS1	100.9	102.2	102.1	101.7±0.57
Dynein+NDEL1	96.6	98.5	97.2	97.4±0.76
Dynein+LIS1+NDEL1	99.1	102.3	100.2	100.6±1.29

Figure 1 Effects of LIS1/NDEL1 on the *in vitro* motor properties of cytoplasmic dynein. (**A**) Dependence of gliding velocity of microtubules (MTs) on the concentration of LIS1 and NDEL1. Molecular ratio is indicated at the bottom. Note: LIS1 displayed dose-dependent inhibition of dynein motility, whereas NDEL1 facilitated dissociation of dynein with MTs. The presence of LIS1 and NDEL1 restored dynein binding with MTs. No translocation was counted due to complete dissociation of dynein at the highest concentration of NDEL1. The *P*-value was calculated using a Student's *t*-test (*$P<0.05$, **$P<0.01$). (**B**) MgATPase activities of cytoplasmic dynein. Each protein was added at a 10-fold stoichiometric amount to the cytoplasmic dynein heavy chain. Left bars: activity without MTs. Right bars: calculated k_{cat} for each protein combination. The *P*-value was calculated using a Student's *t*-test (*$P<0.05$). (**C**) MT-binding assay. The amount of cytoplasmic dynein bound to MTs was indicated in percentage (and s.d.) of total cytoplasmic dynein. LIS1 slightly increased cytoplasmic dynein binding to MTs, whereas NDEL1 reduced the cytoplasmic dynein binding. When both LIS1 and NDEL1 were present, the reduced binding is restored to the level of MTs with LIS1 alone. Three independent experiments were performed, and we found significant difference. Intensity of the band of SDS–PAGE was measured and was normalized as shown at the bottom. The *P*-value was calculated using a Student's *t*-test (*$P<0.05$).

periphery of the cell towards the centrosome along MTs (Vallee, 1991; Vallee and Sheetz, 1996). In addition to a potential role for LIS1 in this normal transport function of dynein, we considered the possibility that LIS1 is essential for dynein transport towards the plus end of MTs. Dynein must be transported first to the plus end of MTs from its site of synthesis to the periphery prior to its loading on MTs to perform minus-end-directed transport. We hypothesized that LIS1 fixes dynein on transportable MT (tMT) fragments, and this dynein–LIS1–tMT complex would then be transported to the plus end en bloc (see Figure 5 below). This possibility is supported by the aberrant distribution of cytoplasmic dynein in the *Lis1* or the *Ndel1* mutant MEF cells. In MEFs with reduced levels of LIS1, dynein appears highly concentrated around the centrosome, associated with peripheral depletion, which was consistent with our earlier results (Sasaki *et al*, 2000; Toyo-oka *et al*, 2003; Yingling *et al*, 2008) (Supplementary Figure 2A–E). In *Ndel1*−/− MEF cells, dynein displayed a similar aberrant distribution as *Lis1*−/− MEF cells, whereas LIS1 appeared broadly distributed in the

cytoplasm with loss of centrosomal accumulation (Sasaki *et al*, 2005) (Supplementary Figure 2A, B and F–I).

To test whether LIS1 and NDEL1 are critical for anterograde and/or retrograde MT dynein transport, we monitored the dynamics of each protein by fluorescence recovery after photobleaching (FRAP) using dorsal root ganglia (DRG) neurons (Supplementary Figure 3A and B). MTs in DRG form a continuous array within the axon, extending from the cell body into the growth cone at its distal tip. Each MT within the array is oriented with its assembly-favoured plus-end directed away from the cell body (Heidemann *et al*, 1981). On the basis of these properties, we were able to define the movement and relationships of each protein. Before FRAP analysis, we defined the effect of simple diffusion in the axon using EGFP protein (Supplementary Figure 3D–G). In contrast to the cell body, diffusion in the axon was extremely low, allowing us to analyse protein transport precisely by FRAP. We also monitored whether GFP-tagged proteins behave similar to endogenous proteins. GFP-tagged proteins displayed similar patterns of immunocytochemistry and similar profiles of sucrose density gradient separation as endogenous proteins, suggesting that GFP-tagged proteins behave similarly with endogenous ones (Supplementary Figure 3H–K). We first examined the movement of GFP-tagged proteins. Kinesin light chain1 (KLC1), as a marker of kinesin-1 displayed only anterograde flux (Supplementary Figure 4A), whereas proteins including dynein, LIS1, NDEL1 displayed bidirectional flux. For tubulin transport, we examined the axon-specific tubulin, tubulin β3 (TUBB3), which displayed dynamic transport within the axon (Wang and Sheetz, 2000; Wang and Brown, 2002) (Supplementary Figure 4B–E). We next characterized anterograde movement using a kinesin inhibitor, AMPPNP. AMPPNP selectively abolished anterograde movement of all of the examined proteins, whereas retrograde movement was almost completely maintained (Supplementary Figure 5; Table I), suggesting that anterograde movement is dependent on kinesin function. We further characterized retrograde movement using a dynein inhibitor, EHNA. EHNA inhibits ATPase activity resulting in the suppression of dynein–MT binding (Bouchard *et al*, 1981; Schliwa *et al*, 1984). Treatment of EHNA suppressed retrograde flux of all of the examined proteins (Supplementary Figure 6; Table I), suggesting that retrograde movement is dependent on dynein function. Interestingly, EHNA did not inhibit anterograde movement of kinesin and TUBB3 (Supplementary Figure 6; Table I), but EHNA clearly inhibited anterograde movement of dynein as well as retrograde movement (Supplementary Figure 6E), suggesting that the interaction between dynein and MTs is essential for anterograde movement of dynein. Even though there is lack of specificity of EHNA as an inhibitor of cytoplasmic dynein, these observations are consistent with our hypothesis regarding anterograde transport of dynein on tMT fragments.

To address LIS1 and NDEL1 function, we initially isolated DRGs from *Lis1* or *Ndel1* conditional knockout mice, and generated DRGs lacking LIS1 or NDEL1 by Cre-mediated gene disruption (Hirotsune *et al*, 1998; Sasaki *et al*, 2005), but functional analysis of LIS1 by genetic inhibition was impossible as the slow loss of LIS1 resulted in death of the DRGs. We therefore analysed the anterograde and retrograde dynamics of each protein by treatment of DRGs with blocking antibodies to LIS1 or NDEL1. We first examined whether blocking antibodies to LIS1 or NDEL1 effectively prevents the binding of each protein to cytoplasmic dynein by a precipitation assay using GST-tagged LIS1/NDEL1 and purified cytoplasmic dynein. Substantial amounts of cytoplasmic dynein were recovered with LIS1 or NDEL by GST–sepharose precipitation. In contrast, the amount of cytoplasmic dynein precipitated with LIS1 or NDEL was dramatically reduced by immunoprecipitation using an anti-LIS1 or an anti-NDEL antibody (Supplementary Figure 7). We also demonstrated that an anti-LIS1 or an anti-NDEL1 antibody clearly abolished the effect of LIS1 or NDEL1 on the motility of cytoplasmic dynein (data not shown). Thus, we concluded that these

Table I Summary of FRAP analysis

EGFPs	AMPPNP (4 mM)[a]	EHNA (1 mM)[b]	Anti-LIS1[a]	Anti-NDEL1[a]
EGFP–DIC1				
Anterograde flux	↓	↓	↓	→
Retrograde flux	→	↓	→	↓ (in the proximal region) → (in the distal region)
EGFP–KLC1				
Anterograde flux	↓	→	→	→
Retrograde flux	—	—	—	—
EGFP–LIS1				
Anterograde flux	↓	→	↓	→
Retrograde flux	→	↓	↓	↓ (in the proximal region) → (in the distal region)
EGFP–NDEL1				
Anterograde flux	↓	→	→	↓
Retrograde flux	→	↓	→	↓
EGFP–TUBB3				
Anterograde flux	↓	→	→	→
Retrograde flux	→	↓	→	→

Horizontal and downward arrows indicate no change compared with the control and reduction of recovery, respectively.
[a]The cells were permeabilized by 8 μM digitonin and incubated with it in the presence of ATP regeneration system (1 mM ATP, 5 mM phosphocreatine and 20 U/ml creatinephosphokinase).
[b]The cells were not permeabilized.

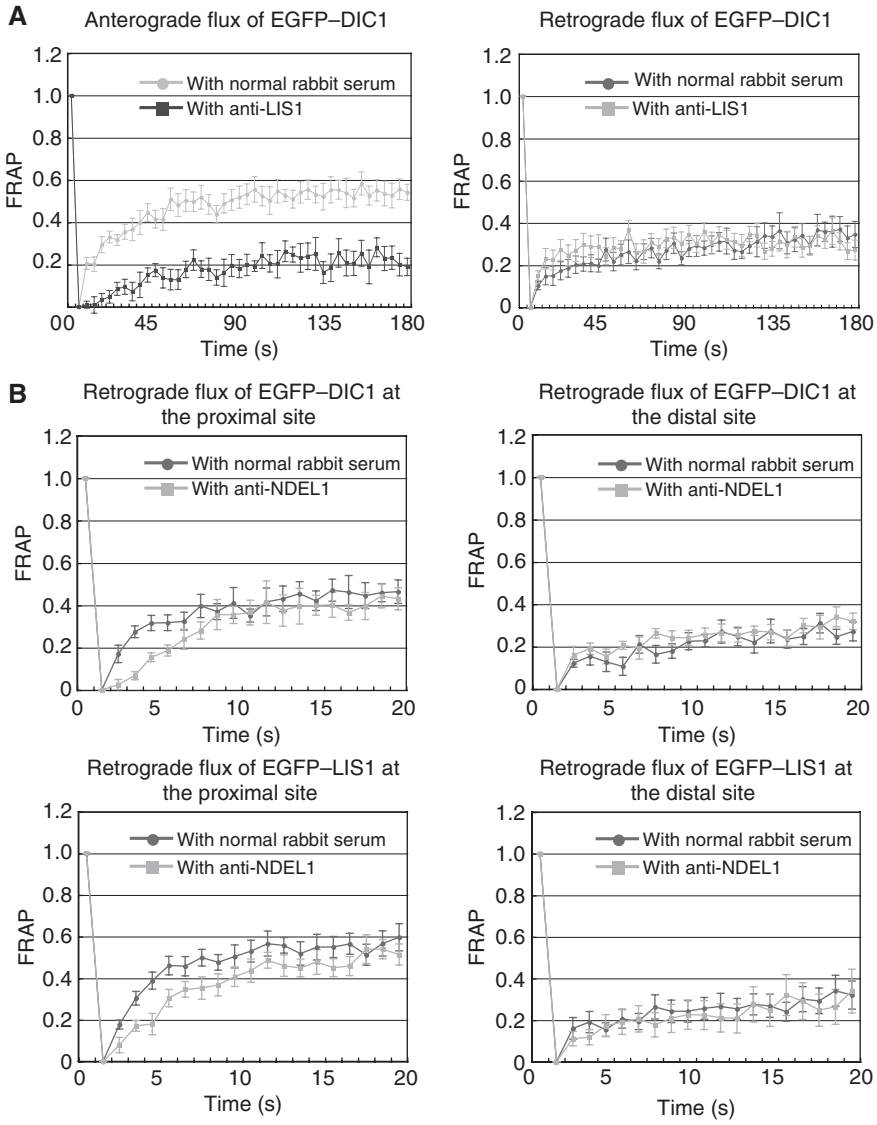

Figure 2 FRAP analysis of dorsal root ganglia (DRG) neuron. FRAP analysis of DRG neuron expressing EGFP-tagged proteins. The graph shows the relative fluorescent recovery directly after bleaching. The prebleach level is normalized to 1.0. (**A**) Dynein recovery in the presence of an anti-LIS1 blocking antibody. (**B**) Retrograde dynein and LIS1 recovery in the presence of AMPPNP and an anti-NDEL1 blocking antibody.

antibodies block LIS1 or NDEL1 function by inhibiting their binding to cytoplasmic dynein. Using these antibodies, we performed FRAP analysis. LIS1 antibody treatment was quite effective in blocking LIS1 movement, and fluorescence recovery of LIS1 was completely abolished (Supplementary Figure 8A). Although LIS1 antibody treatment did not have any obvious effect on the anterograde transport of kinesin, bidirectional transport of TUBB3 and NDEL1, and the retrograde transport of dynein, LIS1 antibody treatment clearly suppressed anterograde transport of dynein (Figure 2A; Table I). These observations suggest that LIS1 is an essential molecule for dynein transport to the plus end of MTs, but it is not required for the retrograde movement of dynein, which is consistent with our biochemical analysis and our hypothesis. We next examined the effect of NDEL1. Treatment with a NDEL1 antibody was quite effective in blocking NDEL1 movement, and fluorescence recovery of NDEL1 was completely abolished (Supplementary Figure 9A). Inhibition of NDEL1 flux did not result in any obvious effect on anterograde movement of the other examined proteins, suggesting that NDEL1 is not required for anterograde movement (Table I). As we found that NDEL1 restores dynein-mediated movement of MTs in the presence of LIS1 (Figure 1B), we hypothesized that NDEL1 was required for dynein movement in the presence of LIS1 and might be needed at the centrosome to generate a steep LIS1 gradient around the centrosome. Therefore, we examined dynein and LIS1 movement in the centre and the periphery of cells (Supplementary Figure 3C), in which LIS1 concentration is high and low, respectively (Supplementary Figure 10). Inhibition of NDEL1 did not suppress the retrograde transport of LIS1 and dynein in the distal region, but clearly the retrograde transport of LIS1 and dynein was suppressed in the region proximal to the cell body (Figure 2B; Table II).

LIS1 is required for the assembly of cytoplasmic dynein with tubulins

To address whether LIS1 is required to assemble cytoplasmic dynein with tubulins, we performed an immunoprecipitation/immunoabsorption assay. DRG neurons were trans-

fected with GFP–DIC1 or a GFP control plasmid, followed by immunoprecipitation using an anti-GFP antibody. GFP and GFP–DIC1 were efficiently precipitated by an anti-GFP antibody (Figure 3A). LIS1 was specifically found in the GFP–DIC1 immunoprecipitate and not in control GFP (Figure 3A). Additionally, kinesin heavy chain (KHC) and TUBB3 were also found in the GFP–DIC1 immunoprecipitate (Figure 3A), suggesting that LIS1, TUBB3 and kinesin-1 all form complexes with cytoplasmic dynein.

We next performed immunoabsorption of the protein extract from DRGs transfected with GFP–DIC by an anti-LIS1 antibody. This anti-LIS1 antibody efficiently removed endogenous LIS1 from the DRG extract (Figure 3B). We then applied immunoprecipitation to the LIS1 protein depleted DRG extract using an anti-GFP antibody, followed by immunoblotting using several antibodies. In sharp contrast with results in the absence of anti-LIS1 antibody (Figure 3A), we were unable to detect precipitates of TUBB3 and KHC with DIC1 in LIS1 absorbed DRG extract (Figure 3B), implying that LIS1 is essential for assembling cytoplasmic dynein with kinesin-1 and tubulins.

We also performed immunoabsorption of NDEL1 in DRGs transfected with GFP–DIC. An anti-NDEL1 antibody also efficiently removed endogenous NDEL1 from the DRG extract (Figure 3C). We immunoprecipitated GFP–DIC from the NDEL1 absorbed DRG extract using an anti-GFP antibody, followed by immunoblotting using given antibodies. Although endogenous NDEL1 was absorbed, we were able to still detect precipitates of TUBB3 and KHC with DIC (Figure 3C), suggesting that NDEL1 is not involved in the formation of complexes of cytoplasmic dynein with kinesin-1 and tubulins.

We performed the same experiments in MEF cells transfected with GFP–DIC or GFP control plasmid, and obtained similar results (Figure 3D–F).

Table II Calculation of $t_{1/2}$(s) of fluorescence recovery in the presence of an anti-NDEL1 antibody

EGFs	Region	Antibody	$t_{1/2} \pm$ s.d.(s)
EGFP–DIC1	Proximal	Normal rabbit serum	2.0 ± 0.30
		Anti-NDEL1	3.8 ± 0.51*
	Distal	Normal rabbit serum	2.6 ± 0.54
		Anti-NDEL1	4.2 ± 1.43
EGFP–LIS1	Proximal	Normal rabbit serum	1.8 ± 0.14
		Anti-NDEL1	3.7 ± 0.43*
	Distal	Normal rabbit serum	2.8 ± 0.78
		Anti-NDEL1	4.2 ± 1.36

*$P<0.05$.
$t_{1/2}$(s) was calculated by Origin Software (Microcal Software Inc., Northampton, MA). The fluorescence recoveries of DIC1 and LIS1 in the distal region were not significantly changed, whereas the recoveries in the proximal region displayed significant reduction.

Co-migration of LIS1, TUBB3 and cytoplasmic dynein

To obtain further evidence for our anterograde transport hypothesis, we examined dynamic colocalization of dynein, LIS1 and soluble tubulin in the axon by visualization of protein movements using confocal time-lapse microscopy. We first examined anterograde movements of mCherry–DIC and EGFP–LIS1 (Figure 4A; Table IIIA), and found that these proteins were colocalized in the same particles. We next examined anterograde movements of mCherry–DIC and EGFP–TUBB3 (Figure 4B; Table IIIA), and found that these proteins were also co-migrating in the same particles. To address whether kinesin-1 mediated the transport of these complexes, we examined co-migration of KLC1 and LIS1 or DIC1. Time-lapse imaging by confocal microscopy clearly revealed co-migration of KLC1 with DIC1 (Figure 4C; Table IIIA) and LIS1 (Figure 4D; Table IIIA) away from the cell body of DRG neurons, indicating that kinesin-1 is likely to be the motor protein responsible for the transport of tMT–LIS1–dynein complex. Combined with our demonstration of an essential role of LIS1 for the plus-end-directed transport of dynein by FRAP and the results of immunoprecipitation/immunoabsorption assay, these results demonstrate that the dynein–LIS1–tMT complex is transported to the plus end of MTs.

In our model, NDEL1 needs to be transported separately from the tMT–LIS1–dynein complex, as NDEL1 reactivates cytoplasmic dynein in the presence of LIS1. To address whether NDEL1 is incorporated into the tMT–LIS1–dynein complex, we examined the frequency of co-migration of LIS1 and NDEL1 with tMTs in the absence or presence of EHNA to dissociate cytoplasmic dynein from all MTs. If NDEL1 is incorporated into the tMT–LIS1–dynein complex, detachment

Figure 3 Immunoprecipitation and immunoabsorption assay. (**A**) Total cell extracts from DRG neurons transiently transfected with either a pGFP vector encoding DIC1 or an empty pGFP vector were immunoprecipitated with an anti-GFP antibody. The input (5%) (pre-IP) and the immunoprecipitates (post-IP) were analysed by SDS–PAGE and western blot with antibodies against the proteins is indicated on the left. Note: LIS1, TUBB3 and KHC1 are precipitated with GFP–DIC1, whereas the GFP control did not result in any precipitation of these proteins. IB with an anti-LIS1 antibody for the GFP control displayed some background due to cross reactivity of the same rabbit serum used rather than any specific signal. (**B**) Immunoabsorption assay to remove endogenous LIS1 by an anti-LIS1 antibody. Upper panel: total cell extracts from DRG neurons were immunoabsorbed with an anti-LIS1 antibody. The input (5%) (pre-IA) and the post-immunoabsorption (post-IA) were analysed by SDS–PAGE and western blot. Note: immunoabsorption efficiently removed endogenous LIS1 from the total extracts. Immunoprecipitation assay by an anti-GFP antibody. Lower panels: LIS1-immunoabsorbed cell extracts from DRG neurons were immunoprecipitated by anti-GFP antibodies. The input (5%) (pre-IP) and the immunoprecipitates (post-IP) were analysed by SDS–PAGE and western blot with antibodies against the proteins indicated on the left. Note: immunoabsorption of LIS1 resulted in the absence of TUBB3 and KHC co-precipitation with GFP–DIC1. (**C**) Immunoabsorption assay to remove endogenous NDEL1 by an anti-NDEL1 antibody. Upper panel: total cell extracts from DRG neurons were immunoabsorbed with an anti-NDEL1 antibody. The input (5%) (pre-IA) and the immunoabsorption (post-IA) were analysed by SDS–PAGE and western blot. Note: immunoabsorption efficiently removed endogenous NDEL1 from the total extracts. Immunoprecipitation assay by an anti-GFP antibody. Lower panels: NDEL1-immunoabsorbed cell extracts from DRG neurons were immunoprecipitated by anti-GFP antibodies. The input (5%) (pre-IP) and the immunoprecipitates (post-IP) were analysed by SDS–PAGE and western blot with antibodies against the proteins indicated on the left. Note: TUBB3 and KHC co-precipitates with GFP–DIC1 in the absence of NDEL1. (**D–F**) MEF cells were transfected with GFP–DIC1 or GFP control plasmid, followed by immunoprecipitation using an anti-GFP antibody. The same immunoprecipitation and immunoabsorption/immunoprecipitation assays were applied to MEF cells, and reproducible results were obtained. Note: in these series of experiments, we used GFP–TUBB5 and an anti-tubulin β antibody instead of GFP–TUBB3 and an anti-tubulin β3 antibody.

of cytoplasmic dynein from TUBB3 by EHNA should reduce the co-migration frequency of NDEL1 and TUBB3. In contrast, if NDEL1 is not incorporated into the tMT–LIS1–dynein complex, detachment of cytoplasmic dynein from TUBB3 by EHNA should not reduce the co-migration frequency of NDEL1 and tubulin. By this way, we can define the cytoplasmic dynein-dependent association of NDEL1 with anterogradely moving tMTs, that is, incorporation of NDEL1 into the tMT–LIS1–dynein complex. First, we examined co-migration frequency between TUBB3 and LIS1 with or without EHNA (Table IIIB). In the absence of EHNA, LIS1 co-migrated with TUBB3 at a high frequency (34/42, 81%), whereas in the presence of EHNA, the frequency of co-migration was reduced to 38% (14/37), suggesting that approximately half of plus-end-directed LIS1 is incorporated into the tMT–Lis1–dynein complex. In sharp contrast, NDEL1 co-migrated with TUBB3 in almost equivalent proportions without (30/55, 55%) or with EHNA (20/36, 56%) (Table IIIB), suggesting that NDEL1 binding is not influenced by the binding of cytoplasmic dynein with TUBB3. These results are highly consistent with our immunoprecipitation and immunoabsorption–immunoprecipitation assays (Figure 3). Taken

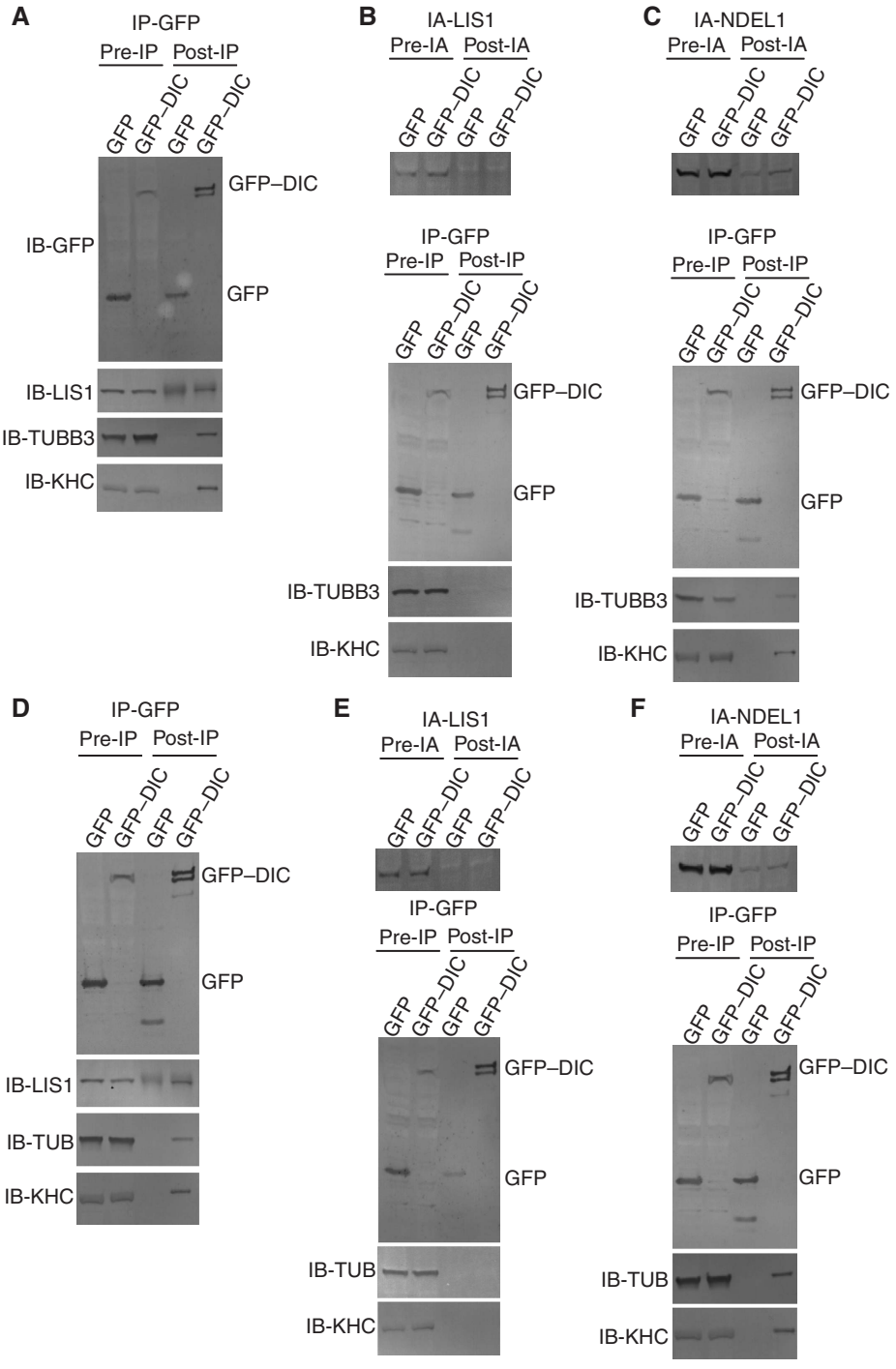

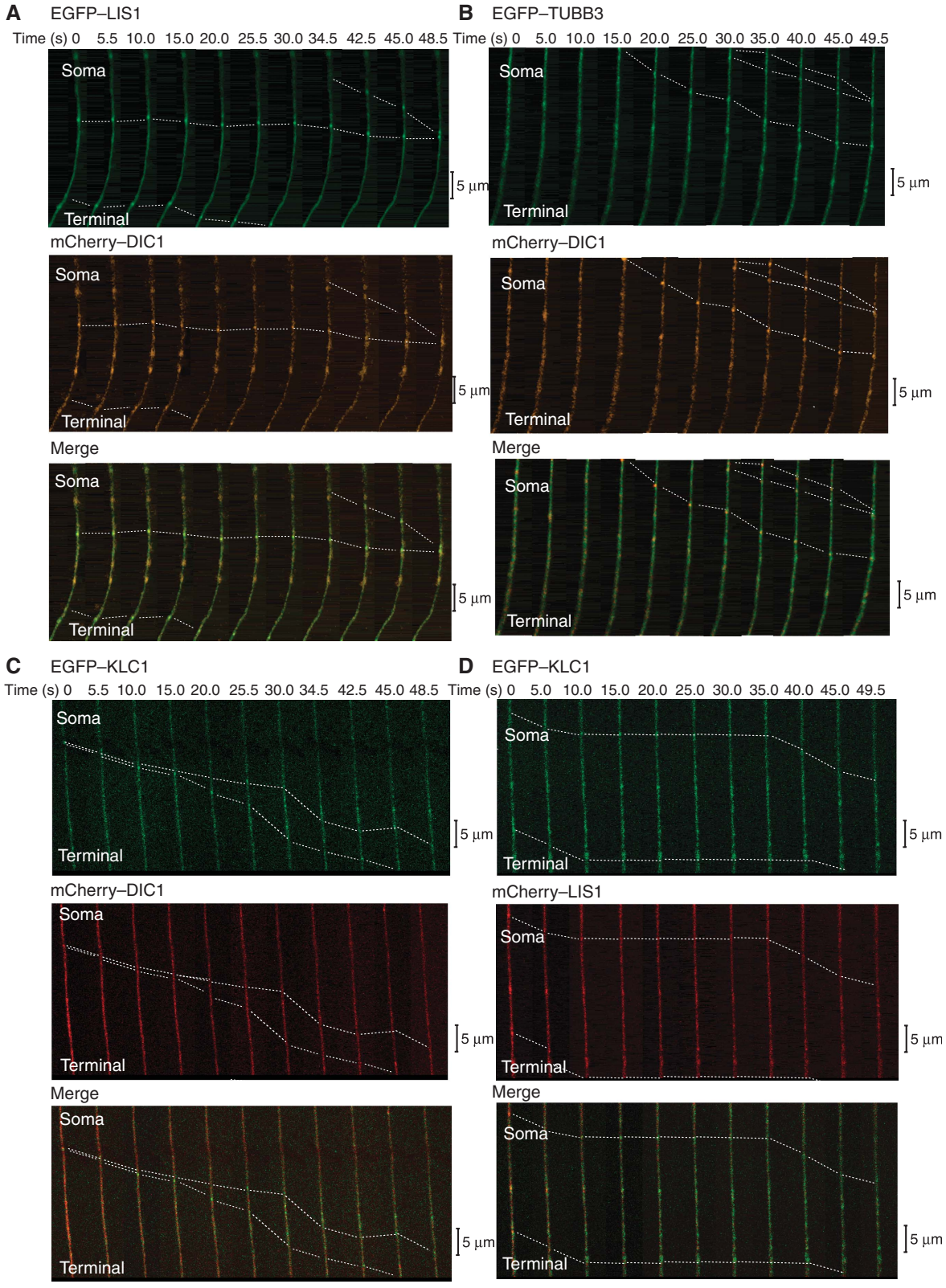

Figure 4 Imaging of movements of LIS1, TUBB3, DIC1 and KLC1 in DRG. Direct visualization of the anterograde movement of fluorescence-tagged proteins in DRG neurons using confocal microscopy. (**A**) EGFP–LIS1 and mCherry–DIC1. (**B**) EGFP–TUBB3 and mCherry–DIC1. (**C**) EGFP–KLC1 and mCherry–DIC. (**D**) EGFP–KLC1 and mCherry–LIS1. Dotted lines indicate dynamic colocalization. Yellow signal indicates colocalized transport. Calculated speed of particles was distributed in 0.5–1.6 μm/s, consistent with the speed of kinesin.

together, we conclude that anterograde co-migration of LIS1 and NDEL1 is not occurring in the tMT–LIS1–dynein complex.

Finally, we addressed whether our model is applicable to the other type of cells, such as MEFs. Given the nature of MT organization in MEF cells, strict definition of the direction of

Table III Examinations of co-migration frequency

(A)

	mChe–DIC1/EGFP–LIS1 complex (%)	Free mChe–DIC1 + free EGFP–LIS1 (%)	*N*
Anterograde migration	20 (61)	13 (39)	33
Retrograde migration	8 (31)	18 (69)	26
	mChe–DIC1/EGFP–TUBB3 complex (%)	Free mChe–DIC1 + free EGFP–TUBB3 (%)	*N*
Anterograde migration	17 (57)	13 (43)	30
Retrograde migration	14 (47)	16 (53)	30
	mChe–NDEL1/EGFP–LIS1 complex (%)	Free mChe–NDEL1 + free EGFP–p50 (%)	*N*
Anterograde migration	15 (26)	42 (74)	57
Retrograde migration	13 (41)	19 (59)	32
	mChe–DIC1/EGFP–KLC1 complex (%)	Free mChe–DIC1 + free EGFP–KLC1 (%)	*N*
Anterograde migration	30 (68)	14 (32)	44
Retrograde migration	—	—	—
	mChe–LIS1/EGFP–KLC1 complex (%)	Free mChe–LIS1 + free EGFP–KLC1 (%)	*N*
Anterograde migration	27 (66)	14 (34)	41
Retrograde migration	—	—	—

(B)

	mChe–LIS1/EGFP–TUBB3 cpmplex (%)	Free mChe–LIS1 + free EGFP–TUBB3 (%)	*N*
EHNA (−)			
Anterograde migration	34 (81)	8 (19)	42
Retrograde migration	24 (78)	7 (22)	31
EHNA (1 mM)			
Anterograde migration	14 (38)	23 (62)	37
Retrograde migration	—	—	—
	mChe–NDEL1/EGFP–TUBB3 complex (%)	Free mChe–NDEL1 + free EGFP–TUBB3 (%)	*N*
EHNA (−)			
Anterograde migration	30 (55)	25 (45)	55
Retrograde migration	8 (26)	23 (74)	31
EHNA (1 mM)			
Anterograde migration	20 (56)	16 (44)	36
Retrograde migration	—	—	—

(A) To characterize the transport of LIS1, NDEL1, TUBB3, KLC1 and DIC, we examined either anterograde or retrograde co-migration frequency in DRG neurons. Co-migration (left), independent migration (middle) and total number of examined signals (right) are indicated. Note: Retrograde co-migration of mCherry–NDEL1 and EGFP–LIS1 is significantly higher than anterograde co-migration. (B) Examination of the EHNA effect (1, absence of EHNA; 2, presence of EHNA) on co-migration frequency of either mCherry–LIS1/EGFP–TUBB3 (upper) or mCherry–NDEL1/EGFP–TUBB3 (lower). Co-migration (left), independent migration (middle) and total number of examined signals (right) are indicated. Note: EHNA clearly diminished co-migration frequency of mCherry–LIS1/EGFP–TUBB3, whereas co-migration frequency of mCherry–NDEL1/EGFP–TUBB3 was unaffected.

transport is technically challenging. Therefore, we solved this problem by measuring the frequency of co-migration of the dynein and tubulin signals in the absence or presence of an anti-LIS1 antibody. As a positive control, we first examined the number of mobile cytoplasmic dynein signals in DRGs (Table IVA). Without an anti-LIS1 antibody, mobile dynein signals were frequently observed moving in both directions, whereas mobile dynein in the anterograde direction was dramatically reduced with an anti-LIS1 antibody. Next, we examined the frequency of co-migration of the dynein and tubulin signals (Table IVA). In the absence of an anti-LIS1 antibody, co-migration was commonly observed during anterograde (60%) and retrograde transport (49%), and total co-migration frequency was 54%. In contrast, in the presence of an anti-LIS1 antibody, the frequency of dynein and tubulin co-migration was clearly reduced in the anterograde direction (19%), whereas the retrograde co-migration frequency was intact (51%). The total co-migration frequency was reduced from 54 to 36% when compared with the control, which is attributable to the selective reduction of anterograde co-migration. We next examined the co-migration of dynein signal and tubulin β-V (TUBB5) signal in MEF cells in the absence or presence of an anti-LIS1 antibody. As separate determination of the transport direction was not possible in MEFs, we measured total co-migration. In the absence of an LIS1 antibody, frequent co-migration of dynein and TUBB5 was observed (66%; Table IVB). By contrast, the co-migration frequency was reduced to 26% in the presence of an anti-LIS1 antibody. On the basis of the DRG results, we reasoned that this reduction is due to the selective dissociation of cytoplasmic dynein with tMTs in anterograde transport, and that LIS1-dependent anterograde transport of cytoplasmic dynein is

Table IV Demonstration of LIS1-dependent anterograde transport of cytoplasmic dynein in MEF cells

(A) mDRG cells	mChe–TUBB3/EGFP–DIC1 complex (%)	Free mChe–TUBB3 + free EGFP–DIC1 (%)	*N*
Anti-LIS1 (−)			
Anterograde migration	21 (60)	14 (40)	35
Retrograde migration	17 (49)	18 (51)	35
Total	38 (54)	32 (46)	70
Anti-LIS1 (+)			
Anterograde migration	7 (19)	29 (81)	36
Retrograde migration	19 (51)	18 (49)	37
Total	26 (36)	47 (64)	73
(B) MEF cells	mChe–TUBB5/EGFP–DIC1 complex (%)	Free mChe–TUBB5 + free EGFP–DIC1 (%)	*N*
Anti-LIS1 (−)	21 (66)	11 (34)	32
Anti-LIS1 (+)	8 (26)	23 (74)	31

To address whether LIS1 mediates anterograde transport of cytoplasmic dynein in other type of cells, we examined the effect of an anti-LIS1 antibody on co-migration frequency of mCherry–TUBB3/EGFP–DIC in DRG neurons (A) and MEF cells (B). Note: The presence of an anti-LIS1 antibody selectively diminished co-migration frequency of mCherry–TUBB3/EGFP–DIC in DRG neurons. Even though determination of direction was not possible in MEF cells, an anti-LIS1 antibody reduced co-migration frequency of mCherry–TUBB3/EGFP–DIC also.

essential for the maintenance of proper dynein distribution in MEF cells. This interpretation is supported by the abnormal accumulation of cytoplasmic dynein around the centrosome (Supplementary Figure 2) in Lis1−/− MEF cells and the disappearance of tubulin and KHC precipitations with DIC1 after immunoabsorption of endogenous LIS1 in MEF cells (Figure 3D–F).

Discussion

In this study, we have demonstrated that LIS1 suppresses motility of MTs by cytoplasmic dynein in a reversible manner, whereas NDEL1 counteracts this suppressive effect. We analysed dynamic movements of cytoplasmic dynein, LIS1 and NDEL1, and found that these proteins are bidirectionally transported. Compared with NDEL1 and cytoplasmic dynein, retrograde flux of LIS1 is significantly smaller than anterograde flux, suggesting that a fraction of LIS1 is degraded after reaching the plus end of MTs. Surprisingly, we also demonstrated that blocking of LIS1 function by an anti-LIS1 antibody severely perturbed anterograde transport of cytoplasmic dynein, whereas retrograde movement of cytoplasmic dynein was not detectably inhibited. In clear contrast, blocking of NDEL1 did not display an obvious effect on anterograde transport, but retrograde transport of cytoplasmic dynein and LIS1 was reduced. This reduction is more noticeable in the vicinity of the cell body, where LIS1 concentration is high. Imaging analysis revealed that cytoplasmic dynein and LIS1 co-migrate towards the plus end of MTs in a complex with tubulins and in a kinesin-1-dependent manner. In this anterogradely moving complex, NDEL1 is not present.

We propose a novel and unique function for dynein regulation by LIS1 and NDEL1 (Figure 5). In our model, LIS1 holds dynein on the tMT to make a complex, which is transported to plus end of MTs. Cytoplasmic dynein appeared clustered around the nucleus in *Lis1*−/− MEF cells (also see Yingling *et al*, 2008), suggesting that Lis1 is required for the movement of cytoplasmic dynein by anterograde transport and consistent with our model. Immunoabsorption of LIS1 from DRG extract resulted in a disruption of the tMT–tubulin complex, suggesting that LIS1 is an essential component to assemble cytoplasmic dynein with tubulins, also in support of this model. Although the use of tMT is a possibility supported by the data, the precise structure of tMTs used for the dynein transport is not clear. However, if tMTs are used, the intensity and shape of EGFP–TUBB3 suggest that the tMT may be oligomeric rather than a common tubular structure as in the cytoskeleton, consistent with a previous report (Terada *et al*, 2000). NDEL1 appears to be responsible for the reactivation of the LIS1–dynein complex at the periphery of the cell. We speculate that NDEL1 allows the minus-end-directed transport of LIS1 by cytoplasmic dynein, and allows LIS1 to establish and maintain a gradient around the

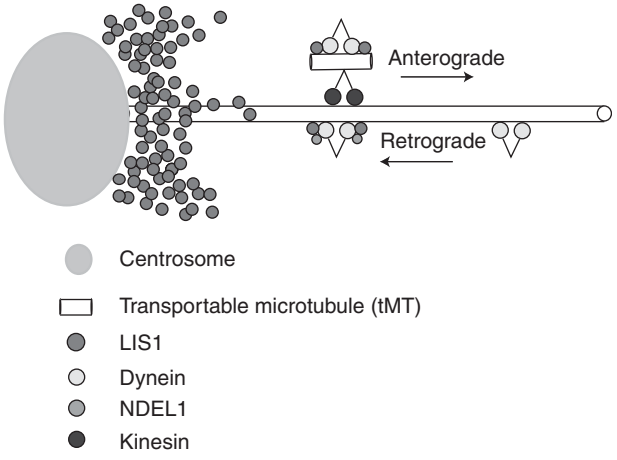

Figure 5 Model of dynein regulation by LIS1 and NDEL1. Schematic presentation of the dynein regulation by LIS1 and NDEL1. LIS1 fixes dynein on tMT (freighter tubulins). This complex is transported to the plus end of cytoskeletal MTs in a kinesin-dependent manner. In contrast, NDEL1 activates the dynein–LIS1 complex, and enables LIS1 protein to accumulate around the centrosome by dynein-dependent transport. Presumably, the generation of the dynein–LIS1–tMT freighter complex requires high concentrations of LIS1 protein around the centrosome.

centrosome, which would be required to generate the dynein–LIS1–tMT complex. *Ndel1−/−* MEF cells displayed homogenous distribution of LIS1 rather than centrosomal accumulation (Sasaki *et al*, 2005), accompanied with perinuclear clustering of cytoplasmic dynein similar to *Lis1−/−* MEF cells, supporting our speculation.

This model is consistent with our observations demonstrating that once *Lis1* is disrupted, plus-end-directed dynein transport is severely impaired, resulting in excessive accumulation around the centrosome associated with peripheral depletion. This unbalanced distribution of cytoplasmic dynein would likely be the causative mechanism of the defect of N–C coupling and nucleokinesis defects displayed by migrating neurons (Tanaka *et al*, 2004). In addition, the depletion of cytoplasmic dynein and LIS1 at the leading edge (Dujardin *et al*, 2003) of migrating neurons likely causes defects at the leading process of migrating neurons. The role of this complex in anterograde transport of cytoplasmic dynein provides an explanation for the normal broad distribution of cytoplasmic dynein are localized in a perinuclear pattern when LIS1 is reduced (Niethammer *et al*, 2000; Sasaki *et al*, 2000; Toyo-oka *et al*, 2003; Yingling *et al*, 2008). It also provides an explanation for the observation that loss of LIS1 results in a reduction of astral MTs, reduction of cortical dynein and impairment of cortical MT capture in mitotic cells (Faulkner *et al*, 2000; Yingling *et al*, 2008). More generally, our model provides a general mechanism for the transport of cytoplasmic dynein to the plus end of cytoskeletal MTs.

The molecular mechanism by which cytoplasmic dynein is activated after reaching the plus end of MTs is not clear at this moment. One possible mechanism is that NDEL1 binds to the tMT–LIS1–dynein complex, and releases cytoplasmic dynein from LIS1 inhibition. Higher frequency of co-migration of LIS1 together with NDEL1 in the cytoplasmic dynein fraction moving in a retrograde manner to minus end of MTs supports this speculation (Table IIIA). Another possibility is that LIS is degraded, as FRAP analysis indicates that the retrograde flux of LIS1 is significantly smaller than anterograde flux. This suggests that as much as half of LIS1 disappears and is likely to be degraded after reaching the plus end of MTs. How LIS1 may be degraded is unknown at this time, but we are currently investigating whether the degradation of LIS1 is a possible mechanism for the activation of cytoplasmic dynein.

Our study also suggests a novel form of soluble tubulin clusters, which may have a different origin and distinct mode of regulation from cytoskeletal MTs. Our imaging analysis suggests that these tubulin clusters exist as stable entities rather than intermediates from the breakdown or remodelling of cytoskeletal MTs. We propose the possibility that these unique tubulin clusters may be distinctly regulated and may also have unique functions such as 'freighter' for the transport of other molecules such as dyneins. By binding to these 'freighter' tMTs in the presence of LIS1, dynein is stably held on the tMTs. The 'freighters' can be used by anterograde kinesin motors to transport stable, inactive dynein in an anterograde manner. These tMTs may also be used more generally to transport other proteins that can attach and be held on MTs in an anterograde manner. The use of such freighter MTs provides a simple and flexible mechanism to transport dynein from inside the cell to the periphery, and may be used more generally for other transportable cargoes.

Materials and methods

Purified and recombinant proteins and dynein motility assay

Cytoplasmic dynein was prepared from porcine brain as described (Bingham *et al*, 1998; Toba and Toyoshima, 2004). The anion exchange column (UnoQ-1; Bio-Rad Laboratories, Hercules, CA)-purified cytoplasmic dynein peaks were pooled in HPLC buffer (35 mM tris(hydroxymethyl)aminomethane), 5 mM $MgSO_4$, 1 mM EGTA, 0.5 mM EDTA, 1 mM DTT, 10 μM ATP, pH 7.2) and supplemented with 24% sucrose. Tubulin was purified from porcine brain (Sloboda and Rosenbaum, 1982). Samples of cytoplasmic dynein and tubulins were flash-frozen and stored in liquid nitrogen. GST-tagged recombinant proteins of LIS1 and NDEL1 were expressed in High-Five insect cells using the Bac-To-Bac baculovirus system based on the manufacturer's protocol (Invitrogen, Carlsbad, CA).

In vitro MT gliding assays were performed as described earlier (Vale and Toyoshima, 1988) and modified (Toba and Toyoshima, 2004). Before the motility assays, the dynein preparation was further purified to remove the dynein that could bind to MTs in an ATP-insensitive manner. Dynein was added with 1 mM ATP, 40 μM taxol and 0.5 mg/ml MTs and allowed to stand. After ultracentrifugation, the dynein in the supernatant was used for motility assays. For the first type of experiments, dynein was mixed with LIS1/NDEL1 (final concentration of dynein 35 μg/ml) for 5 min on ice, and then introduced into the observation chamber. Excess LIS1/NDEL1 molecules that were not associated with dynein were washed away during the subsequent procedures. The velocities of 30 translocating MTs were measured in each condition. The means ± standard deviation of the velocities are shown. For the second type of experiments, the chamber was set up by applying LIS1/NDEL1 in sequence. Dynein (35 μg/ml) was initially absorbed onto the glass surface, and the unabsorbed dynein was washed away. Thereafter, LIS1/NDEL1 was introduced into the chamber. The molar ratios were calculated to indicate the stoichiometry of LIS1/NDEL1 to the dynein heads in the mixture or solution introduced into the chamber.

Dynein MgATPase assay

The MgATPase activities of dynein (final concentration 60 μg/ml) were determined at 25°C in HPLC buffer containing 1 mM ATP. The released inorganic phosphate was measured by the malachite green method (Kodama *et al*, 1986). Determination of the k_{cat} values was typically performed at six or more concentrations of MTs. The MT-activated ATPase activities were obtained by subtracting the activity without MTs from that with MTs and fitted by nonlinear regression to the hyperbolic expression. The means ± s.d. of the activities from three separate experiments are indicated as phosphate released per second per molecule.

MT-binding assay

Dynein was mixed with LIS1, NDEL1 or both in the presence of 10 mM ATP. The final concentration of dynein was 50 μg/ml. The mixing molar ratio of the dynein heavy chain to LIS1/NDEL1 was 1:10. MAP-depleted tubulin (0.3 mg/ml) and 40 μM taxol (Sigma) were added to the mixture, and then incubated for 5 min at room temperature. After dynein binding, the MTs were collected by centrifugation at 200 000 *g* for 10 min at room temperature using a 100.2 rotor in an Optima TLX ultracentrifuge (Beckman Coulter Inc.). The supernatants and pellets were separated and subjected to electrophoresis. The images of the gels were digitized and the bands were quantified by densitometry.

Sedimentation assay and co-sedimentation assay

To examine co-sedimentation of cytoplasmic dynein with LIS1 or NDEL1, dynein was mixed with LIS1, NDEL1 or both, and loaded onto a 15–30% sucrose density gradient (150 000 *g*, 20 h, 2°C, P50S2 rotor; Hitachi, Japan) in K-buffer (20 mM PIPES-KOH, 50 mM KCl, 20 mM β-mercaptoethanol, 10% glycerol, 0.1% NP-40) in the presence of 1 mM AMP-PNP. The final concentration of dynein was 50 μg/ml. The mixing molar ratio of the dynein heavy chain to LIS1/NDEL1 was 1:10. After centrifugation, the gradients were divided into 22 fractions of equal volume. All the sucrose density gradient fractions were analysed by SDS–PAGE. The gels were stained with silver and quantified by densitometry. For immuno-

blotting, an anti-GST antibody (A-5800; Molecular Probes Inc., Eugene, OR) was used.

DRG preparation, culture and FRAP

DRGs from postnatal mice were dissociated using a previously described method (Lindsay, 1988). During dissociation of cells, D-MEM was used with 10% heat-inactivated bovine serum, 200 ng/ml 2.5 s mNGF (Sigma) and 5 μM uridine/deoxyfluorouridine (Sigma). The cells were plated onto poly-D-lysine-coated dishes (MatTek) and cultured in the above medium for 48–72 h. DRGs were transfected with vectors to express various proteins immediately after dissection using the Basic Nucleofector kit for primary neurons (Amaxa Biosystems). FRAP analyses were performed to extended axons from DRGs using the 510 META system (Carl Zeiss) 48–72 h after transfection as described (Mochizuki *et al*, 2001). Position, length and grey-scale pixel values were measured on digitized confocal images. Fluorescence recovery $t_{1/2}$ was estimated by measuring the average grey-scale pixel values using the line-scan function. All data were reported as mean ± s.d.

Imaging of protein movements

For tracking mCherry- and EGFP-fused proteins in axons of living DRG neurons and MEF cells, an IX81 inverted microscope (Olympus) equipped with an FV-1000 confocal imaging system (Olympus) was used.

Immunostaining

MEF cells or DRG neurons were fixed with 4% paraformaldehyde in 0.1 M sodium phosphate buffer (pH 7.4) for 20 min at room temperature. Fixed cells were incubated with 0.2% Triton X-100/TBS to be permeabilized for 10 min at room temperature, followed by blocking treatment. Here, 5% BSA/0.2% Tween20/TBS or milk-based blocking reagent, BLOCKACE (Dainippon Sumitomo Pharma, Osaka, Japan) supplemented with 2% FCS was used for blocking an antiphosphorylated or antiunphosphorylated protein antibody, respectively. After the blocking, we incubated the cells with various antibodies at 4°C overnight or for 1 h at room temperature. We used the antibodies at the following dilutions in blocking solution: rabbit anti-NDEL1 (Sasaki *et al*, 2000), rabbit anti-LIS1 mouse monoclonal anti-γ-tubulin (Sigma), mouse monoclonal anti-β-tubulin (Sigma) and anti-tubulin β3 mouse monoclonal antibody (Genzyme). After washing three times with 0.1% Tween20/TBS for 10 min each, cells were treated with various secondary antibodies in blocking solution for 60 min at room temperature. We used the following secondary antibodies: Alexa546-labelled donkey anti-mouse IgG or anti-rabbit IgG (Molecular Probes); AlexaFluor488-labelled donkey anti-mouse IgG or anti-rabbit IgG (Molecular Probes). We visualized nuclei with 300 nM DAPI and mounted the cells with 90% glycerol/PBS.

Sucrose gradient centrifugation and immunoprecipitation experiments

Whole brain extracts for sucrose gradient centrifugation experiments were prepared from brain tissues of C57BL/6 mice 14 days after birth. Briefly, mouse brains were collected and homogenized in 1 × BRB80 buffer (80 mM potassium-PIPES, 1 mM $MgCl_2$, 1 mM EGTA, 1 mM DTT, pH 6.8) with 0.2% NP-40, followed by centrifugation for 3 min at 15 000 r.p.m. at room temperature. Mouse brain extracts were fractionated on 14 ml of 10–30% sucrose gradients in 1 × BRB80 buffer by centrifugation for 3 h at 28 000 r.p.m. in an P28S rotor (Hitachi) at 20°C. For immunoprecipitation experiments, DRG neurons were lysed in immunoprecipitation buffer (20 mM Tris–HCl, 100 mM NaCl, 1 mM DTT, 0.2% NP-40), followed by centrifugation for 3 min at 15 000 r.p.m. at room temperature. Immunoprecipitation experiments were carried out from DRG neuron total cell extracts by using an anti-GFP rabbit polyclonal antibody (Clontech) bound to protein G-sepharose (GE Healthcare) in immunoprecipitation buffer for 1 h at room temperature. Following five washes with the same immunoprecipitation buffer, bound proteins were eluted by boiling in SDS–PAGE sample buffer. The antibodies used are as follows: anti-LIS1 antibody, anti-KHC mouse monoclonal antibody (Chemicon) or anti-tubulin β3 mouse monoclonal antibody (Genzyme). For immunoabsorption, DRG neuron total cell extracts were incubated with 25 μg of anti-LIS1 antibody or anti-NDEL1, which had been conjugated with protein G-sepharose (GE Healthcare), at room temperature for 1 h. Supernatant was further subjected to immunoprecipitation analysis.

Supplementary data

Supplementary data are available at *The EMBO Journal* Online (http://www.embojournal.org)

Acknowledgements

We thank Yoshihiko Funae, Hiroshi Iwao, Toshio Yamauch, Masami Muramatsu, Yoshitaka Nagai and Michiyuki Matsuda for generous support and encouragement. This study was supported by Grant-in-Aid for Scientific Research from the Ministry of Education, Science, Sports and Culture of Japan from the Ministry of Education, Science, Sports and Culture of Japan to Shinji Hirotsune. This study was also supported by The RIKEN BioResource Center grant for R&D on genetically modified mouse strains, The Sagawa Foundation for Promotion of Cancer Research, The Cell Science Research Foundation, The Japan Spina Bifida & Hydrocephalus Research Foundation, Takeda Science Foundation and The Hohansha Foundation to Shinji Hirotsune, and NIH grants NS41030 and HD47380 to Anthony Wynshaw-Boris.

References

Bingham JB, King SJ, Schroer TA (1998) Purification of dynactin and dynein from brain tissue. *Methods Enzymol* **298:** 171–184

Bouchard P, Penningroth SM, Cheung A, Gagnon C, Bardin CW (1981) erythro-9-[3-(2-Hydroxynonyl)]adenine is an inhibitor of sperm motility that blocks dynein ATPase and protein carboxylmethylase activities. *Proc Natl Acad Sci USA* **78:** 1033–1036

Dobyns WB, Curry CJ, Hoyme HE, Turlington L, Ledbetter DH (1991) Clinical and molecular diagnosis of Miller–Dieker syndrome. *Am J Hum Genet* **48:** 584–594

Dobyns WB, Reiner O, Carrozzo R, Ledbetter DH (1993) Lissencephaly. A human brain malformation associated with deletion of the LIS1 gene located at chromosome 17p13. *JAMA* **270:** 2838–2842

Dujardin DL, Barnhart LE, Stehman SA, Gomes ER, Gundersen GG, Vallee RB (2003) A role for cytoplasmic dynein and LIS1 in directed cell movement. *J Cell Biol* **163:** 1205–1211

Efimov VP, Morris NR (2000) The LIS1-related NUDF protein of *Aspergillus nidulans* interacts with the coiled-coil domain of the NUDE/RO11 protein. *J Cell Biol* **150:** 681–688

Faulkner NE, Dujardin DL, Tai CY, Vaughan KT, O'Connell CB, Wang Y, Vallee RB (2000) A role for the lissencephaly gene LIS1 in mitosis and cytoplasmic dynein function. *Nat Cell Biol* **2:** 784–791

Feng Y, Olson EC, Stukenberg PT, Flanagan LA, Kirschner MW, Walsh CA (2000) LIS1 regulates CNS lamination by interacting with mNudE, a central component of the centrosome. *Neuron* **28:** 665–679

Gupta A, Tsai LH, Wynshaw-Boris A (2002) Life is a journey: a genetic look at neocortical development. *Nat Rev Genet* **3:** 342–355

Heidemann SR, Landers JM, Hamborg MA (1981) Polarity orientation of axonal microtubules. *J Cell Biol* **91:** 661–665

Hirotsune S, Fleck MW, Gambello MJ, Bix GJ, Chen A, Clark GD, Ledbetter DH, McBain CJ, Wynshaw-Boris A (1998) Graded reduction of Pafah1b1 (Lis1) activity results in neuronal migration defects and early embryonic lethality. *Nat Genet* **19:** 333–339

Kodama T, Fukui K, Kometani K (1986) The initial phosphate burst in ATP hydrolysis by myosin and subfragment-1 as studied by a modified malachite green method for determination of inorganic phosphate. *J Biochem (Tokyo)* **99:** 1465–1472

Lee WL, Oberle JR, Cooper JA (2003) The role of the lissencephaly protein Pac1 during nuclear migration in budding yeast. *J Cell Biol* **160:** 355–364

Lei Y, Warrior R (2000) The *Drosophila* Lissencephaly1 (DLis1) gene is required for nuclear migration. *Dev Biol* **226:** 57–72

Lindsay RM (1988) Nerve growth factors (NGF, BDNF) enhance axonal regeneration but are not required for survival of adult sensory neurons. *J Neurosci* **8:** 2394–2405

Mesngon MT, Tarricone C, Hebbar S, Guillotte AM, Schmitt EW, Lanier L, Musacchio A, King SJ, Smith DS (2006) Regulation of cytoplasmic dynein ATPase by Lis1. *J Neurosci* **26:** 2132–2139

Mochizuki N, Yamashita S, Kurokawa K, Ohba Y, Nagai T, Miyawaki A, Matsuda M (2001) Spatio-temporal images of growth-factor-induced activation of Ras and Rap1. *Nature* **411:** 1065–1068

Morris SM, Albrecht U, Reiner O, Eichele G, Yu-Lee LY (1998) The lissencephaly gene product Lis1, a protein involved in neuronal migration, interacts with a nuclear movement protein, NudC. *Curr Biol* **8:** 603–606

Niethammer M, Smith DS, Ayala R, Peng J, Ko J, Lee MS, Morabito M, Tsai LH (2000) NUDEL is a novel Cdk5 substrate that associates with LIS1 and cytoplasmic dynein. *Neuron* **28:** 697–711

Paschal BM, King SM, Moss AG, Collins CA, Vallee RB, Witman GB (1987) Isolated flagellar outer arm dynein translocates brain microtubules *in vitro*. *Nature* **330:** 672–674

Rivas RJ, Hatten ME (1995) Motility and cytoskeletal organization of migrating cerebellar granule neurons. *J Neurosci* **15:** 981–989

Sasaki S, Mori D, Toyo-oka K, Chen A, Garrett-Beal L, Muramatsu M, Miyagawa S, Hiraiwa N, Yoshiki A, Wynshaw-Boris A, Hirotsune S (2005) Complete loss of Ndel1 results in neuronal migration defects and early embryonic lethality. *Mol Cell Biol* **25:** 7812–7827

Sasaki S, Shionoya A, Ishida M, Gambello MJ, Yingling J, Wynshaw-Boris A, Hirotsune S (2000) A LIS1/NUDEL/cytoplasmic dynein heavy chain complex in the developing and adult nervous system. *Neuron* **28:** 681–696

Schliwa M, Ezzell RM, Euteneuer U (1984) erythro-9-[3-(2-Hydroxynonyl)]adenine is an effective inhibitor of cell motility and actin assembly. *Proc Natl Acad Sci USA* **81:** 6044–6048

Shu T, Ayala R, Nguyen MD, Xie Z, Gleeson JG, Tsai LH (2004) Ndel1 operates in a common pathway with LIS1 and cytoplasmic dynein to regulate cortical neuronal positioning. *Neuron* **44:** 263–277

Sloboda RD, Rosenbaum JL (1982) Purification and assay of microtubule-associated proteins (MAPs). *Methods Enzymol* **85** (Part B)**:** 409–416

Tanaka T, Serneo FF, Higgins C, Gambello MJ, Wynshaw-Boris A, Gleeson JG (2004) Lis1 and doublecortin function with dynein to mediate coupling of the nucleus to the centrosome in neuronal migration. *J Cell Biol* **165:** 709–721

Terada S, Kinjo M, Hirokawa N (2000) Oligomeric tubulin in large transporting complex is transported via kinesin in squid giant axons. *Cell* **103:** 141–155

Toba S, Toyoshima YY (2004) Dissociation of double-headed cytoplasmic dynein into single-headed species and its motile properties. *Cell Motil Cytoskeleton* **58:** 281–289

Toyo-Oka K, Sasaki S, Yano Y, Mori D, Kobayashi T, Toyoshima YY, Tokuoka SM, Ishii S, Shimizu T, Muramatsu M, Hiraiwa N, Yoshiki A, Wynshaw-Boris A, Hirotsune S (2005) Recruitment of katanin p60 by phosphorylated NDEL1, an LIS1 interacting protein, is essential for mitotic cell division and neuronal migration. *Hum Mol Genet* **14:** 3113–3128

Toyo-oka K, Shionoya A, Gambello MJ, Cardoso C, Leventer R, Ward HL, Ayala R, Tsai LH, Dobyns W, Ledbetter D, Hirotsune S, Wynshaw-Boris A (2003) 14-3-3epsilon is important for neuronal migration by binding to NUDEL: a molecular explanation for Miller–Dieker syndrome. *Nat Genet* **34:** 274–285

Vale RD, Toyoshima YY (1988) Rotation and translocation of microtubules *in vitro* induced by dyneins from *Tetrahymena cilia*. *Cell* **52:** 459–469

Vallee R (1991) Cytoplasmic dynein: advances in microtubule-based motility. *Trends Cell Biol* **1:** 25–29

Vallee RB, Sheetz MP (1996) Targeting of motor proteins. *Science* **271:** 1539–1544

Vallee RB, Wall JS, Paschal BM, Shpetner HS (1988) Microtubule-associated protein 1C from brain is a two-headed cytosolic dynein. *Nature* **332:** 561–563

Wang L, Brown A (2002) Rapid movement of microtubules in axons. *Curr Biol* **12:** 1496–1501

Wang Z, Sheetz MP (2000) The C-terminus of tubulin increases cytoplasmic dynein and kinesin processivity. *Biophys J* **78:** 1955–1964

Yingling J, Youn YH, Darling D, Toyo-Oka K, Pramparo T, Hirotsune S, Wynshaw-Boris A (2008) Neuroepithelial stem cell proliferation requires LIS1 for precise spindle orientation and symmetric division. *Cell* **132:** 474–486